

# NUCLEON AND NUCLEAR SPIN STRUCTURE FUNCTIONS <sup>a</sup>

S. SCOPETTA

*Departament de Fisica Teorica, Universitat de València, E-46100 Burjassot  
(València), Spain*

A.Yu. UMINIKOV

*INFN, Sezione di Perugia, via A. Pascoli, I-06100 Perugia, Italy.*

C. CIOFI DEGLI ATTI

*Department of Physics, University of Perugia, and INFN, Sezione di Perugia,  
I-06100 Perugia, Italy.*

L.P. KAPTARI

*Bogoliubov Lab. of Theor. Phys., Joint Institute for Nuclear Research, Dubna,  
Russia.*

Nuclear effects in polarized inelastic electron scattering off polarized  $^3He$  and polarized  $^2H$  are discussed; in the resonance region, Fermi motion effects are found to be much larger than in deep inelastic scattering. It is shown that improperly describing nuclear dynamics would lead to the extraction of unreliable neutron spin structure functions; on the other hand side, simple and workable equations, relating the Gerasimov – Drell – Hearn Integral for the neutron to the corresponding quantity for  $^3He$  and  $^2H$ , are proposed. Nuclear effects in the recent E143 data are estimated by a proper procedure.

## 1 Introduction

The measurement of the polarized nucleon Spin Structure Functions (SSF)  $g_1$  and  $g_2$  in the resonance region allows one to check the helicity structure of the photon – nucleon coupling between the Deep Inelastic Scattering (DIS) region and the real photon limit<sup>1</sup>. Recently it has been proposed at TJNAF to study the SSF in a wide range of energy ( $0.2 \text{ GeV} \leq \nu \leq 3 \text{ GeV}$ ) and momentum ( $0.15 \text{ GeV}^2 \leq Q^2 \leq 2 \text{ GeV}^2$ ) transfers, for both the proton<sup>2</sup> and the neutron, using in the latter case polarized  $^2H$  and  $^3He$  targets<sup>3,4</sup>.

For a hadronic target  $A$ , the SSF  $g_1^A(\nu, Q^2)$  and  $g_2^A(\nu, Q^2)$  are experimentally obtained by measuring longitudinal and transverse asymmetries<sup>5</sup>. A

---

<sup>a</sup>Invited talk at the Conference “Perspectives in Hadronic Physics”, Trieste, May 12-16, 1997. Presented by S. Scopetta

relevant quantity related to the SSF's  $g_{1(2)}$  is the following integral

$$I^A(Q^2) = \frac{8\pi^2\alpha}{m} \int_{\nu_{th}}^{\infty} \frac{d\nu}{\nu} \frac{\left(1 + \frac{Q^2}{\nu^2}\right)}{K} \mathcal{G}_1^A(\nu, Q^2), \quad (1)$$

where  $\nu_{th} = (Q^2 + 2m_\pi m + m_\pi^2)/2m$  is the threshold energy for the pion-electroproduction off the nucleon,  $m$  is the nucleon mass,  $m_\pi$  is the pion mass,  $K$  is the photon flux,  $\alpha$  is the fine structure constant and  $\mathcal{G}_1^A(\nu, Q^2)$  reads as:

$$\mathcal{G}_1^A(\nu, Q^2) = \frac{1}{\left(1 + \frac{Q^2}{\nu^2}\right)} \left( g_1^A(\nu, Q^2) - \frac{Q^2}{\nu^2} g_2^A(\nu, Q^2) \right). \quad (2)$$

Two features of  $\mathcal{G}_1^A(\nu, Q^2)$  have to be mentioned: (i) when multiplied by the quantity  $-\frac{2\nu}{M_A}(1 + \frac{Q^2}{\nu^2})$ ,  $M_A$  being the target mass, it coincides with the usual transverse response,  $R_{T'}$  (see e.g.<sup>6</sup>); and (ii) in the DIS limit ( $Q^2 \rightarrow \infty$ ,  $\nu \rightarrow \infty$ ,  $Q^2/\nu$  fixed),  $\mathcal{G}_1^A$  coincides with the SSF,  $g_1^A(\nu, Q^2)$ .

For any spin  $\frac{1}{2}$  hadronic target, the SSF  $g_1^A$  and  $g_2^A$  read as follows<sup>5</sup>

$$g_1^A(\nu, Q^2) = \frac{M_A K}{8\pi^2\alpha(1 + \frac{Q^2}{\nu^2})} \left[ \Delta\sigma^A(\nu, Q^2) + \frac{2\sqrt{Q^2}}{\nu} \sigma_{TL}^A(\nu, Q^2) \right], \quad (3)$$

$$g_2^A(\nu, Q^2) = \frac{M_A K}{8\pi^2\alpha(1 + \frac{Q^2}{\nu^2})} \left[ \frac{2\nu}{\sqrt{Q^2}} \sigma_{TL}^A(\nu, Q^2) - \Delta\sigma^A(\nu, Q^2) \right], \quad (4)$$

where  $\Delta\sigma^A(\nu, Q^2) = \sigma_{1/2}^A(\nu, Q^2) - \sigma_{3/2}^A(\nu, Q^2)$ ,  $\sigma_{1/2(3/2)}^A(\nu, Q^2)$  is the cross section for photon – hadron scattering with total helicity  $1/2$  ( $3/2$ ),  $\sigma_{TL}^A(\nu, Q^2)$  is the transverse – longitudinal interference cross section. Thus Eq. (2) becomes:

$$\mathcal{G}_1^A(\nu, Q^2) = \frac{M_A K}{8\pi^2\alpha(1 + \frac{Q^2}{\nu^2})} \left[ \sigma_{1/2}^A(\nu, Q^2) - \sigma_{3/2}^A(\nu, Q^2) \right]. \quad (5)$$

For a nucleon target ( $A = N$ ,  $N = n$  or  $p$ ), the integral  $I^A$  coincides with the Gerasimov – Drell – Hearn (GDH) integral,  $I_{GDH}^N(Q^2)$ , which, in the real photon limit, gives the GDH Sum Rule<sup>7</sup>:

$$I_{GDH}^N(Q^2 = 0) = \int_{\nu_{th}}^{\infty} \frac{d\nu}{\nu} \left( \sigma_{1/2}^N(\nu, Q^2 = 0) - \sigma_{3/2}^N(\nu, Q^2 = 0) \right) = -\frac{2\pi^2\alpha}{m^2} \kappa_N^2$$

$$\simeq \begin{cases} -0.53 & GeV^{-2} \text{ for protons} \\ -0.60 & GeV^{-2} \text{ for neutrons} \end{cases} \quad (6)$$

where  $\kappa_N$  is the anomalous magnetic moment of the nucleon.

An important observation<sup>8</sup> can be made about the  $Q^2$  evolution of  $I_{GDH}^N$ . Since in the large  $Q^2$  limit  $\mathcal{G}_1^N$  coincides with  $g_1^N$ , one can evaluate (1) for the proton, using the results<sup>9</sup> at  $Q^2 \simeq 10 \text{ GeV}^2$ , which gives  $I_{GDH}^p(Q^2) \simeq 0.14/Q^2$ . This result, if compared with (6), provides evidence of a sharp modification in the helicity structure of the  $\gamma p$  coupling between the real photon limit (6) and the DIS region, which lead to a change of sign of  $I_{GDH}^p(Q^2)$  at some value of  $Q^2$ . In order to understand this behavior, much theoretical work has been produced<sup>10,11</sup>, both in the real photon limit and at finite values of  $Q^2$ . The electroexcitation of nucleon resonances is evidently the main reason for this evolution of the integral,  $I_{GDH}^p(Q^2)$ . Therefore, experimental investigation of the low- $Q^2$  evolution of  $I_{GDH}^N$  is of great relevance, in particular for the neutron, for which several analyses of the available unpolarized data for photoproduction and low- $Q^2$  electroproduction disagree with the prediction (6), while similar estimates seem to give the correct value for the proton.

Since  $\mathcal{G}_1^n(\nu, Q^2)$  will be extracted from experimental data on  ${}^2\vec{H}$  and  ${}^3\vec{He}$ , corrections due to nuclear effects have to be introduced. The goal of this talk is to illustrate the relevance of these corrections in the resonance region. Our results for  ${}^3\vec{He}$  and  ${}^2\vec{H}$  are presented in the following two sections<sup>12,13</sup>. The recent deuteron data of the E143 collaboration<sup>14</sup> are used as an example to test the method proposed in<sup>15</sup> for the extraction of the neutron SSF from the nuclear ones.

## 2 The process ${}^3\vec{He}(\vec{e}, e')X$ in the resonance region

Using the convolution model for the nuclear SSF  $g_{1(2)}^A$  described in<sup>6,16,17</sup>, we obtain<sup>12</sup>

$$\begin{aligned} \mathcal{G}_1^A(\nu, Q^2) = & \sum_{N=p,n} \int dz \int dE \int d\vec{p} \frac{m}{E_p} \frac{m\nu}{p \cdot q} \left\{ \mathcal{G}_1^N(\nu', Q^2) P_{\parallel}^N(\vec{p}, E) \right. \\ & \left. + T^N(\vec{p}, E, Q^2) \right\} \delta \left( z + \frac{m^2 - p \cdot p}{2m\nu} - \frac{q \cdot p}{m\nu} \right), \end{aligned} \quad (7)$$

where  $E$  is the removal energy of a nucleon with momentum  $\vec{p}$ ,  $p \equiv (M_A - \sqrt{(E + M_A - m)^2 + |\vec{p}|^2}, \vec{p})$  is the nucleon 4-momentum,  $q$  is the 4-momentum transfer,  $E_p = \sqrt{m^2 + |\vec{p}|^2}$ ,  $P_{\parallel}^N(\vec{p}, E)$  and  $T^N(\vec{p}, E, Q^2)$  are related to the elements of the 2x2 matrix, which represents the spin dependent spectral function<sup>6</sup>.

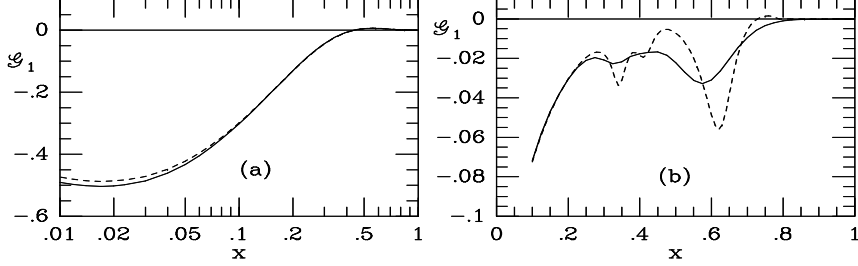


Figure 1:  $\mathcal{G}_1^{^3He}$  in DIS ( $Q^2 = 10 \text{ GeV}^2$ ) (a)<sup>16</sup>, and in resonance ( $Q^2 = 1 \text{ GeV}^2$ ) (b) regions, obtained by considering Fermi motion and binding (full). The dashed curve represents the same functions obtained considering the proton and neutron effective polarization in  $^3He$  as the only relevant nuclear effects (Eq. (12)).

The elements of this matrix are

$$P_{\sigma,\sigma',\mathcal{M}}^N(\vec{p}, E) = \sum_{f_{A-1}} \langle \vec{p}, \sigma; \psi_{A-1}^f | \psi_{J\mathcal{M}} \rangle \langle \psi_{J\mathcal{M}} | \psi_{A-1}^f; \vec{p}, \sigma' \rangle \times \delta(E - E_{A-1}^f + E_A) \quad (8)$$

where  $|\psi_{J\mathcal{M}}\rangle$  is the ground state of the polarized target nucleus,  $|\psi_{A-1}^f\rangle$  is the eigenstate of the (A-1) nucleon system with eigenvalue  $E_{A-1}^f$ , and  $|\vec{p}, \sigma\rangle$  is the plane wave describing the struck nucleon in continuum. The relevant quantity is  $P_{||}^N(\vec{p}, E) = P_{\frac{1}{2}\frac{1}{2}, \frac{1}{2}}^N(\vec{p}, E) - P_{-\frac{1}{2}-\frac{1}{2}, \frac{1}{2}}^N(\vec{p}, E)$ , i. e. the difference between the spectral functions with nucleon spin parallel or antiparallel to the nucleus spin. It provides the effective nucleon polarizations  $p_N$  produced by the  $S'$  and  $D$  waves in the ground state of  $^3He$ :

$$p_N = \int dE \int d\vec{p} P_{||}^N(\vec{p}, E) . \quad (9)$$

The spectral function of<sup>6</sup> gives  $p_{p(n)} = -0.030$  (0.88), in agreement with world calculations on the three body systems<sup>18</sup>,  $p_{p(n)} = -0.028 \pm 0.004$  ( $0.86 \pm 0.02$ ).

The term  $T^N(\vec{p}, E, Q^2)$  depends also upon  $P_{\frac{1}{2}-\frac{1}{2}, \frac{1}{2}}^N(\vec{p}, E)$ , as well as upon a proper combination of the SSF's  $g_1$  and  $g_2$ <sup>16</sup>. However, it is of the order  $|\vec{p}/m|$ , and thus gives a very small contribution both in the DIS<sup>16</sup> as well as in the present calculation of the resonance region. For this reason it will be omitted hereafter. The quantity  $\mathcal{G}_1^N$  which appears in  $\mathcal{G}_1^{^3He}$  (Eq. (7)) is defined in terms of the polarized electroproduction cross-sections  $\sigma_{1/2(3/2)}^N$  (cf. Eq. (5)). Since the first few data for  $\mathcal{G}_1^N$  appeared very recently<sup>14</sup>, we use a theoretical model<sup>11</sup>, where the contributions of the resonances  $P_{33}(1232)$ ,  $D_{13}(1520)$ ,

$S_{11}(1535)$  and  $F_{15}(1680)$  have been parametrized using the existing experimental data for unpolarized electroproduction. Other resonant states have been added using the predictions of a single quark transition model, and the single pion Born term background has also been included. Using the above models for  $P_{\parallel}^N(\vec{p}, E)$  and  $\mathcal{G}_1^N$ , we have calculated  $\mathcal{G}_1^{^3He}$  in the resonance region. The results are presented in Fig. 1, where they are compared with the results for the DIS limit<sup>16</sup>. In the latter case  $\mathcal{G}_1^A(\nu, Q^2) = g_1^A(\nu, Q^2) = \frac{M_A K}{8\pi^2 \alpha} [\sigma_{1/2}^A(\nu, Q^2) - \sigma_{3/2}^A(\nu, Q^2)]$ , and Eq. (7) reduces to the well-known convolution formula:

$$g_1^A(x, Q^2) = \sum_N \int_x^{M_A/m} dz \frac{1}{z} g_1^N\left(\frac{x}{z}, Q^2\right) G^N(z) , \quad (10)$$

where  $G^N(z)$  is the light-cone momentum distribution

$$G^N(z) = \int dE \int d\vec{p} P_{\parallel}^N(\vec{p}, E) \delta\left(z - \frac{p^+}{M}\right) \quad (11)$$

with  $p^+ = (p^0\nu - \vec{p}\cdot\vec{q})/|\vec{q}|$  being the light-cone momentum component. Fig. 1 shows that in the DIS case the following equation

$$\mathcal{G}_1^{^3He}(x, Q^2) \approx 2p_p \mathcal{G}_1^p(x, Q^2) + p_n \mathcal{G}_1^n(x, Q^2) , \quad (12)$$

approximates very well the convolution formula, at least for  $x \leq 0.8$ <sup>16</sup>. The same does not hold in the resonance region, where nuclear effects turn out to be important, with the Fermi motion significantly broadening and damping the peaks associated with the excitation of the prominent resonant states. Therefore, Eq. (12) can be considered as a workable formula for extracting the DIS  $\mathcal{G}_1^n(x, Q^2)$  from experimental data on  $\mathcal{G}_1^{^3He}(x, Q^2)$ , but in the resonance region it appears to be of little help. We stress that the importance of nuclear effects in the resonance region is a well-known feature of the unpolarized scattering as well. Nevertheless, we have found that the proton contribution to the nuclear  $\mathcal{G}_1^{^3He}(x, Q^2)$  is not large, and therefore  $^3He$  is a good effective polarized neutron target also in the resonance region.

Let us now discuss the role of nuclear effects on the integral Eq. (1). In Fig. 2 the integral, calculated placing Eq. (7) in Eq. (1), is compared with the following expression

$$\tilde{I}^{^3He}(Q^2) = 2p_p I^p(Q^2) + p_n I^n(Q^2) , \quad (13)$$

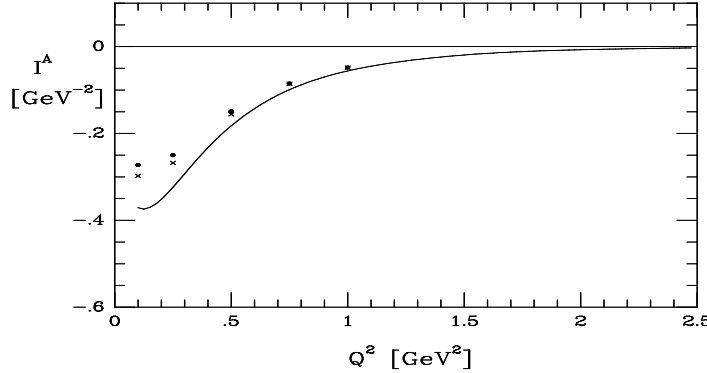


Figure 2: The integral  $I^{^3He}(Q^2)$ , Eq. (5) (dots), compared with the approximation (13) (crosses) and with  $I^n(Q^2)^{11}$  (solid line).

which represents the integral (1) within the assumption that Fermi motion and binding can be disregarded and that nuclear effects in polarized  ${}^3He$  are only due to the effective nucleon polarizations. It can be seen that Eq. (13) approximates Eq. (1) with an accuracy better than 5%. From the same figure it can also be seen that, because of the effective nucleon polarizations, the integral (1) for the free neutron predicted by<sup>11</sup>, noticeably differs from  $I^{^3He}(Q^2)$ . Thus the nuclear structure effects are very large in the nuclear SSF  $\mathcal{G}_1^A(\nu, Q^2)$  (cf. Fig. 1 (b)), but in the integral  $I^{^3He}(Q^2)$  these effects can be approximately accounted for by the effective nucleon polarizations (cf. Fig. 2). This result is understood<sup>12</sup> by performing a series expansion of the r.h.s. of Eq. (7) in the variable  $z$  around the non relativistic value  $z = 1$ .

To sum up, we have shown that in the resonance region  $\mathcal{G}_1^{^3He}(x, Q^2) \neq p_n \mathcal{G}_1^n(x, Q^2) + 2p_p \mathcal{G}_1^p(x, Q^2)$ , but the integrals of the two quantities are very similar.

### 3 The process ${}^2\vec{H}(\vec{e}, e')X$ in the resonance region

The nucleon contribution to the deuteron structure functions is usually calculated by weighting the amplitude of electron scattering on the nucleon with the wave function of nucleon in the deuteron (for recent developments see e.g.<sup>20,21</sup> and references therein). For the SSF the most important effects are the Fermi motion and the depolarizing effect of the D-wave. Additional effects, such as off-mass-shell effects or nucleon deformation, are found to be small<sup>22</sup>. For

finite values of  $Q^2$  and  $\nu$ , Eq. (2) for the deuteron reads as follows<sup>13</sup>

$$\begin{aligned} \mathcal{G}_1^D(x, Q^2) &= \int \frac{d^3\mathbf{p}}{(2\pi)^3} \frac{m\nu}{pq} \mathcal{G}_1^N(x^*, Q^2) \left(1 + \frac{\xi(x, Q^2)p_3}{m}\right) \\ &\quad \times (\Psi_D^{M+}(\mathbf{p}) S_z \Psi_D^M(\mathbf{p}))_{M=1} \\ &= \int_{z_{min}(x, Q^2)}^{z_{max}(x, Q^2)} \frac{dz}{z} \mathcal{G}_1^N(x/z, Q^2) \vec{f}_D(z, \xi(x, Q^2)), \end{aligned} \quad (14)$$

where  $\mathcal{G}_1^N = (\mathcal{G}_1^p + \mathcal{G}_1^n)/2$  is the isoscalar nucleon response given by Eq. (5) and  $\Psi_D^M(\mathbf{p})$  the deuteron wave function with spin projection  $M$ . In the rest-frame of the deuteron, with  $\mathbf{q}$  opposite the z-axis, the kinematical variables are defined as follows:

$$pq = \nu(p_0 + \xi(x, Q^2)p_3), \quad p_0 = m + \epsilon_D - \mathbf{p}^2/2m, \quad (15)$$

$$\xi \equiv q_3/\nu = |\mathbf{q}|/\nu = \sqrt{1 + 4m^2x^2/Q^2}, \quad Q^2 \equiv -q^2, \quad x^* = Q^2/2pq, \quad (16)$$

where  $\epsilon_D = -2.2246$  MeV is the deuteron binding energy.

The limits  $z_{min(max)}(x, Q^2)$  are defined to provide an integration over the physical region of momentum in (14) and to take into account the pion production threshold in the virtual photon-virtual nucleon scattering. Eq. (14) has the correct limit in DIS. In this case:  $\xi(x, Q^2) \rightarrow 1$ ,  $z_{min} \rightarrow x$ ,  $z_{max} \rightarrow M_D/m$ , and the usual convolution formula for the deuteron SSF  $g_1^D(x, Q^2)$  is recovered<sup>20,21</sup>:

$$g_1^D(x, Q^2) = \int_x^{M_D/m} \frac{dz}{z} g_1^N(x/z, Q^2) \vec{f}_D(z). \quad (17)$$

(cf. Eq. (12) for the  ${}^3He$  case). Equation (17) defines the spin-dependent “effective distribution of the nucleons”,  $\vec{f}_D$ , which describes the bulk of nuclear effects in  $g_1^D$ . The main features of the distribution function,  $\vec{f}_D(z)$ , are a sharp maximum at  $z = 1 + \epsilon_D/2m \approx 0.999$  and a normalization given by  $(1 - 3/2P_D)$  ( $P_D$  being the weight of the D-wave in the deuteron). As a result in the region of medium values of  $x \sim 0.2 - 0.6$  the deuteron SF  $g_1^D(x)$  is slightly suppressed by Fermi motion and binding effects, compared to  $(1 - 3/2P_D) \times g_1^N(x)$ . However, the magnitude of this suppression is small ( $\sim 1\%$ ) and this is why it is phenomenologically acceptable to extract the neutron SF from the deuteron and proton data by making use of the following approximate formula:

$$g_1^D(x, Q^2) \approx \left(1 - \frac{3}{2}P_D\right) (g_1^n(x, Q^2) + g_1^p(x, Q^2))/2, \quad (18)$$

(cf. Eq. (14) for the  ${}^3He$  case). In addition, when integrated over  $x$ , eqs. (17) and (18) give exactly the same result ( $\Gamma = \int dx g_1(x)$ ), i.e.

$$\Gamma_D(Q^2) = \left(1 - \frac{3}{2}P_D\right)(\Gamma_n(Q^2) + \Gamma_p(Q^2))/2, \quad (19)$$

which allows one to obtain *exactly* the integral of the neutron SF  $\Gamma_n$  knowing the deuteron and proton integrals, without solving (17).

As in the  ${}^3He$  case, the equations at finite values of  $Q^2$  and  $\nu$  are more sophisticated than the corresponding equations in the deep inelastic limit. In particular, Eq. (14) does not represent a “convolution formula” in the usual sense, since the effective distribution function  $\tilde{f}_D$  and the integration limits are also functions of  $x$ . This circumstance immediately leads to the conclusion that, in principle, when integrals of the SF are considered, the effective distribution can not be integrated out to get a factor similar to  $(1 - 3/2P_D)$  in (19). Another interesting feature of Eq. (14) is the  $Q^2$ -dependence of  $\tilde{f}_D$  and  $z_{min,(max)}(x, Q^2)$ . If we again limit ourselves to the discussion of the integrals of SF, one concludes that the  $Q^2$ -dependence of such an integral is governed by both the QCD-evolution of the nucleon SF and the kinematical  $Q^2$ -dependence of the effective distribution of nucleons. Thus, in principle, in the non-asymptotic regime, equation (19), does not hold.

We have performed a realistic calculation of Eq. (14). As in the  ${}^3He$  case, in our numerical estimates we have evaluated  $\mathcal{G}_1^N$  in (14) using the elementary cross sections for the proton and neutron given in<sup>11</sup>. Using the Bonn potential model for the deuteron wave function<sup>23</sup>, we have carried out a realistic calculation of  $\mathcal{G}_1^D(x, Q^2)$ , (14), in the region of nucleon resonances. In Fig. 3, the obtained  $\mathcal{G}_1^D(x, Q^2)$  at  $Q^2 = 1.0 \text{ GeV}^2$ , is compared with the input of the calculation, i.e. the isoscalar nucleon response,  $\mathcal{G}_1^N(x, Q^2)$ . It can be seen that the role of nuclear effects in the resonance region is much larger (up to  $\sim 50\%$  in the maxima of the resonances), than in the deep inelastic regime ( $\sim 7 - 9\%$ , depending upon the models<sup>20,21</sup>, with resulting  $\sim 6 - 7\%$  from the depolarization factor  $(1 - 3/2P_D)$  and  $\sim 1 - 2\%$  from the binding effects and Fermi motion). As in the  ${}^3He$  case, such a drastic effect is a consequence of the presence of the narrow resonance peaks in the nucleon  $\mathcal{G}_1^N(x, Q^2)$ .

Let us now discuss the role of nuclear corrections in the analysis of the integrals of the SSF, such as the GDH Integral.

An important observation has been made in DIS, namely the *exact* formula (17) and the *approximate* formula (18) give the same result for the integral of the neutron structure function,  $g_1^n(x, Q^2 \gg m^2)$  (see eq. (19)). The applicability of the approximate formula in DIS is based on the conservation of the norm of the distribution  $\tilde{f}(z)$  by the convolution formula (17). This circumstance

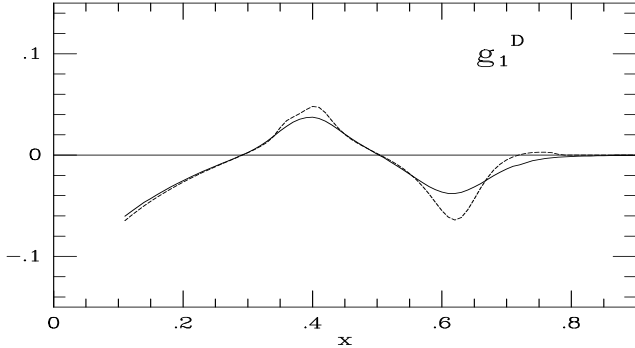


Figure 3:  $\mathcal{G}_1(x, Q^2)$  at  $Q^2=1$  GeV $^2$  for the deuteron SF (solid line), compared with the corresponding quantity for the isoscalar nucleon (dotted line), used as input in the calculation of eq. (14).

can not be immediately extended to the case of the resonance region, since: (i) the convolution is broken in eq. (14) and (ii) the normalization of the function  $\vec{f}(z, x, Q^2)$  is different from the one of  $\vec{f}(z)$ . The integral of the distribution  $\vec{f}(z, x, Q^2)$  represents the “effective number” of nucleons “seen” by the virtual photon in the process when the virtual photon is absorbed by the nucleon and at least one pion is produced in the final state (it is less than 1 at low  $Q^2$  and  $x \rightarrow x_{max}$ ).

However, the use of the formula (19) in the resonance region gives results numerically very close to the integration of the exact equation (14). As explained in<sup>13</sup>, this is a consequence of the smallness of the effects breaking the convolution in eq. (14).

We have found that the integrals of the SF, such as the GDH Sum Rule, can be estimated with accuracy better than 3% by the simple formula (19) which is also valid in deep inelastic region.

#### 4 Neutron SSF from nuclear data

At this point, we have observed that nuclear effects in the resonance region are very specific and therefore approximate formulae, such as (12) for  ${}^3He$  or (18) for  ${}^2H$ , do not work even for crude extraction of the neutron response. Obviously, another method of extracting should be used.

In ref.<sup>15</sup> a rigorous procedure of solving eq. (17) for the unknown neutron SSF has been proposed and applied in the deep inelastic region. It has been shown that this method, which works for both spin-independent and

spin-dependent SSF, in principle allows one to extract the neutron SSF exactly, requiring only the analyticity of SSF. It can also be applied by a minor modification to the extraction of the SSF at finite  $Q^2$ . Such a procedure can be applied both to  ${}^2H$  and  ${}^3He$  targets; here only the deuteron case will be discussed.

The basic idea is to replace the integral equation (14) by a set of linear algebraic equations,  $KG_N = G_D$ , where  $K$  is a square matrix (depending upon the deuteron model),  $G_D$  is a vector containing the available  $\mathcal{G}_1^D$  data and  $G_N$  is a vector of unknown solutions. Changing the integration variable in (14),  $\tau = x/z$ , we get

$$\mathcal{G}_1^D(x, Q^2) = \int_{\tau_{min}(x, Q^2)}^{\tau_{max}(x, Q^2)} d\tau \mathcal{G}_1^N(\tau, Q^2) \frac{1}{\tau} \vec{f}_D(x/\tau, \xi(x, Q^2)), \quad (20)$$

where  $\tau_{min}(x, Q^2) = x/z_{max}(x, Q^2)$ ,  $\tau_{max}(x, Q^2) = x_{max}(Q^2)/z_{min}(x, Q^2)$  and  $x_{max}(Q^2)$  is defined by the pion production threshold in virtual photon-nucleon scattering. Let us assume that  $\mathcal{G}_1^D$  has been measured experimentally in the interval  $(x_1, x_2)$  and that a reasonable parametrization for it can be obtained in this interval. Then, dividing both intervals  $(x_1, x_2)$  and  $(\tau_{min}, \tau_{max})$  into  $N$  small parts, one may write:

$$\mathcal{G}_1^D(x_i, Q^2) \approx \sum_{j=1}^N \mathcal{G}_1^N(\tilde{\tau}_j, Q^2) \int_{\tau_j}^{\tau_{j+1}} \frac{1}{\tau} \vec{f}_D(x_i/\tau, Q^2) d\tau, \quad i = 1 \dots N, \quad (21)$$

where  $\tilde{\tau}_j = \tau_{min} + h(j - 1/2)$  and  $h = (\tau_{max} - \tau_{min})/N$ . Equation (21) is already explicitly of the form  $G_D = KG_N$ , therefore usual linear algebra methods can be applied to solve it.

Note that the range of variation of  $\tau$  is larger than the one for  $x$ . Therefore the experimental knowledge of  $\mathcal{G}_1^D$  in the interval  $(x_1, x_2)$  provides information about the neutron in a wider interval (for example, in deep inelastic regime  $\tau_{min} \approx x/2$  and  $\tau_{max} = 1$ ). However, extracting information beyond the interval  $\tilde{\tau}_{min} = x_1$  to  $\tilde{\tau}_{max} = x_2$  is almost impossible in view of the structure of the kernel of eq. (20) and the kinematical condition of planned experimental data <sup>15</sup>. We have to redefine the kernel of eq. (20) to incorporate new limits of integration  $\tilde{\tau}_{min} = x_1$  and  $\tilde{\tau}_{max} = x_2$ <sup>15</sup>. The experimental errorbars of the nuclear data can be related to errors in the extracted structure function of the nucleon.

To show how this procedure works in practice, we have obtained  $\mathcal{G}_1^N$  of the isoscalar nucleon solving Eq. (14), using in the left hand side an analytical fit of

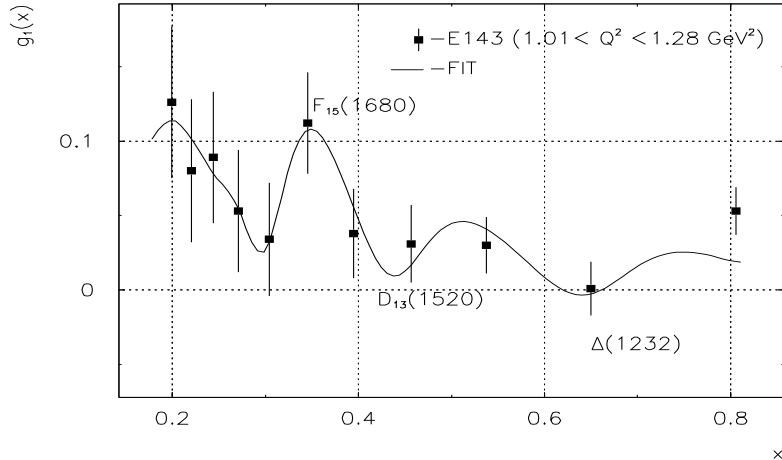


Figure 4: The analytical fit of the deuteron E143 data<sup>14</sup> used as input in our example of extraction

one set of the recent E143 deuteron data<sup>14</sup> (corresponding to  $1.01 \leq Q^2 \leq 1.28$   $\text{GeV}^2$ , see Fig. 4). It should be noticed that in the experimental analysis the difference between  $g_1$  and  $\mathcal{G}_1$  (cf. Eq. (2)) has been neglected, and therefore the data refer to the SSF  $g_1^D$  of the deuteron. Resonance structures corresponding to the three main resonances have been included in obtaining the fit. However, no further physical assumptions have been made, and the behavior of the fitting curve is basically forced by the data, whose errorbars are large. Therefore, our analysis is only a crude estimate of the possible nuclear effects, and presently it should be considered as an example of how the extraction method could be applied. Once we have assumed that our fit describes the nuclear data fairly well, Eq. (14) can be solved using the method described in this section. The results of the calculation are shown in Figs. 5 and 6. It can be seen that nuclear effects are large, and that the extraction procedure allows one to discover features of the isoscalar nucleon SSF which, due to nuclear effects, are not apparent in the initial nuclear SSF. The neutron SSF could be obtained by subtracting the proton data from the isoscalar SSF, and provided the errorbars on  $\mathcal{G}_1^D$  are reduced, this method will provide us with a reliable neutron SSF.

## 5 Conclusions

We have shown that the effects of nuclear structure in the extraction of the neutron SSF in the resonance region are much more important than in DIS.

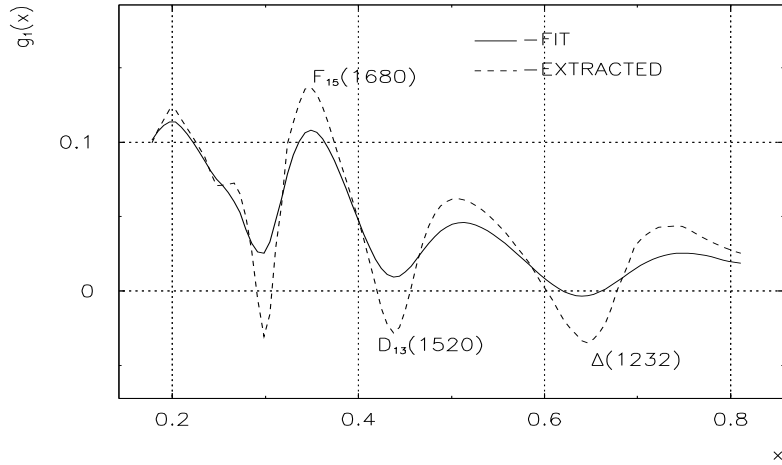


Figure 5: The extracted isoscalar nucleon SSF (dashed line) compared with our fit of the E143 data<sup>14</sup> (full line), used as input in our calculation.

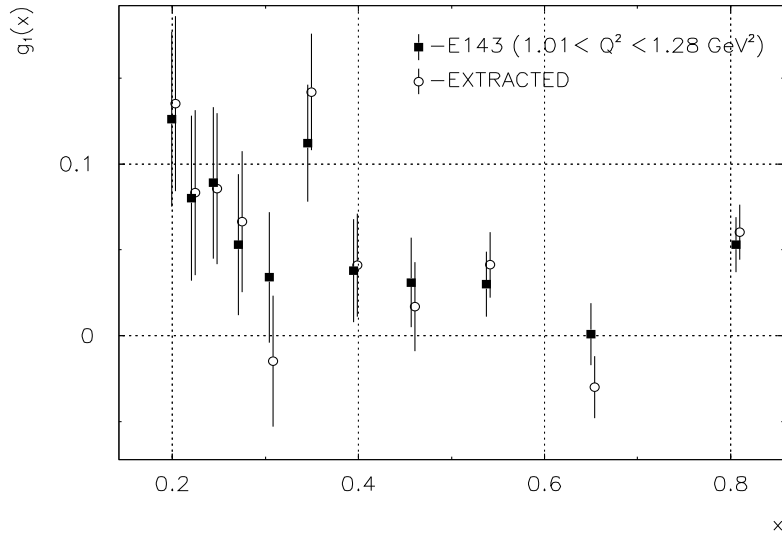


Figure 6: The extracted “data” of the isoscalar nucleon SSF (open circles) compared with the experimental deuteron ones (filled squares). The extracted points have been slightly shifted, in order to distinguish their errorbars from the experimental ones.

We have explained how the correct neutron SSF can be firmly extracted from the combined deuteron and proton data. As for the integrals of the SSF, the estimates are easier, and they can be carried out by using the simple procedure similar to the DIS case.

### Acknowledgments

Two of us (S.S. and A.U.) thanks the Organizers of the Conference for the invitation, and S.S. thanks the TMR programme of the European Commission ERB FMRX-CT96-008 for partial financial support.

### References

1. D. Drechsel, *Prog. Part. Nucl. Phys.* 34 (1995) 181.
2. V. Burkert *et al.*, "Measurement of Polarized Structure Functions in Inelastic Electron Proton Scattering using the CEBAF Large Acceptance Spectrometer", CEBAF Proposal No. 91 – 023.
3. S. E. Kuhn *et al.*, "The Polarized Structure Function  $g_1^n$  and the  $Q^2$  dependence of the Gerasimov – Drell – Hearn Sum Rule for the Neutron", CEBAF proposal No. 93 – 009.
4. Z.E. Meziani, "Measurement of the Neutron ( ${}^3He$ ) Spin Structure Function at Low  $Q^2$ ; a Connection between the Bjorken and the DHG Sum Rules", CEBAF Proposal No. 94 – 010.
5. B.L. Ioffe, V.A. Khoze and L.N. Lipatov, "Hard Processes", North-Holland, New York (1983).
6. C. Ciofi degli Atti, E. Pace, and G. Salmè, *Phys. Rev.* C46 (1992) R1591; 51 (1995) 1108.
7. S.D. Drell and A.C. Hearn, *Phys. Rev. Lett.* 162 (1966) 1520; S.B. Gerasimov, *Yad. Fiz.* 2 (1965) 839 [*Sov. J. Nucl. Phys.* 2 (1966) 589].
8. M. Anselmino, B.L. Ioffe and E. Leader, *Sov. J. Nucl. Phys.* **49** (1989) 136.
9. J. Ashman *et al.*, *Phys. Lett.* B206 (1988) 364; *Phys. Lett.* B328 (1990) 1.
10. I. Karliner, *Phys. Rev.* D7 (1973) 2712; R. Workman and R. Arndt, *Phys. Rev.* D45 (1992) 1789; D. Drechsel and M.M. Giannini, *Few–Body Systems* 15 (1993) 99.
11. V. Burkert and Zhujun Li, *Phys. Rev.* D47 (1993) 46; V. Burkert and B. L. Ioffe, *Phys. Lett.* B296 (1992) 223.
12. C. Ciofi degli Atti and S. Scopetta *Phys. Lett.* B404 (1997) 223.

13. C. Ciofi degli Atti, L.P. Kaptari, S. Scopetta and A.Yu. Umnikov, *Phys. Lett.* B376 (1996) 309; Proceedings of the 9<sup>th</sup> Amsterdam miniconference “Electromagnetic studies of the deuteron”, NIKHEF, Amsterdam, February 1-2, 1996; nucl-th 9602026.
14. K. Abe et al. (E143 Collaboration), *Phys. Rev. Lett.* 78 (1977) 815.
15. L.P. Kaptari, F. Khanna and A.Yu Umnikov, *Z. Phys.* A348 (1994) 211.
16. C. Ciofi degli Atti, S. Scopetta, E. Pace, and G. Salmè, *Phys. Rev.* C48 (1993) R968.
17. R.W. Schultze and P.U. Sauer, *Phys. Rev.* C48 (1993) 38.
18. J.L. Friar et al., *Phys. Rev.* C42 (1990) 2310.
19. L.P. Kaptari, A.Yu. Umnikov *Phys. Lett.* B240 (1990) 203.
20. A.Yu. Umnikov, L.P. Kaptari, K.Yu. Kazakov and F. Khanna, *Phys. Lett.* B334 (1994) 163; L.P.Kaptari, A.Yu. Umnikov, C. Ciofi degli Atti, S.Scopetta and K.Kazakov, *Phys. Rev.* C51 (1995) 52.
21. W. Melnitchouk, G. Piller and A. Thomas, *Phys. Lett.* B346 (1995) 165; S. Kulagin, W. Melnitchouk, G. Piller and W. Weise, *Phys. Rev.* C52 (1995) 932.
22. W. Melnitchouk, A.W. Schreiber and A.W. Thomas, *Phys. Rev.* D49 (1994) 1183; A.Yu. Umnikov, L.P. Kaptari, and F. Khanna, *Phys. Rev.* C53 (1996) 351.
23. R. Machleid, K. Holinde and Ch. Elster, *Phys. Rep.* 149 (1987) 1.